Arabian Journal of Chemistry (2021) **14**, 103396

King Saud University

Arabian Journal of Chemistry

www.ksu.edu.sa
www.sciencedirect.com

ORIGINAL ARTICLE

Synthesis and *In-silico* Simulation of Some New Bis-thiazole Derivatives and Their Preliminary Antimicrobial Profile: Investigation of Hydrazonoyl Chloride Addition to Hydroxy-Functionalized Bis-carbazones

Refaie M. Kassab [a], Sobhi M. Gomha [a,b], Sami A. Al-Hussain [c,*], Ahmed S. Abo Dena [d,e], Marwa M. Abdel-Aziz [f], Magdi E.A. Zaki [c], Zeinab A. Muhammad [d,*]

[a] *Department of Chemistry, Faculty of Science, Cairo University, Giza 12613, Egypt*
[b] *Department of Chemistry, Faculty of Science, Islamic University in AlmadinahAlmonawara, Almadinah Almonawara 42351, Saudi Arabia*
[c] *Department of Chemistry, Faculty of Science, Imam Mohammad Ibn Saud Islamic University (IMSIU), Riyadh 11623, Saudi Arabia*
[d] *Departmentof Pharmaceutical Chemistry, National Organization for Drug Control and Research (NODCAR), Giza 12311, Egypt*
[e] *Faculty of Oral and Dental Medicine, Future University in Egypt (FUE), New Cairo, Egypt*
[f] *Regional Center for Mycology and Biotechnology, Al-Azhar University, Cairo 11754, Egypt*

Received 19 June 2021; accepted 17 August 2021
Available online 28 August 2021

KEYWORDS

Carbazone;
Hydrazonoyl chlorides;
Bis-thiazoles;
Antimicrobial;
DFT;
In-silico studies

Abstract Two new series of *bis*-thiazoles **6a-f** and *bis*-thiazolones **9a-d** were prepared via reacting bis-thiosemicarbazone **3** with hydrazonoyl chloride derivatives **4a-f** and **7a-d,** respectively, in dioxane under basic conditions. Another group of *bis*-thiazole derivatives **12a-h** was prepared by reacting bis-thiosemicarbazone **3** with each of phenacyl bromide derivatives **10a-h** under a similar reaction protocol. A plausible mechanism was proposed. Structural elucidation of the new products was established using both elemental and spectrometric/spectroscopic analyses. Structural, electronic, and the pharmacological characteristics of the prepared molecules were investigated with DFT calculations. Antibacterial and antifungal activities of the new *bis*-thiazoles were screened and compared with vancomycin and amphotericin B as antimicrobial standards. Molecular docking

* Corresponding author.
E-mail addresses: sahussain@imamu.edu.sa (S.A. Al-Hussain), zeinab.a.muhammad@gmail.com (Z.A. Muhammad).
Peer review under responsibility of King Saud University.

Production and hosting by Elsevier

https://doi.org/10.1016/j.arabjc.2021.103396

studies on the promising candidate compounds, with the lowest minimum inhibitory concentrations (MIC), were performed with SAP2 of *C. albicans* and FabI of *S. aureus* and *P. aeruginosa*.

Contents

1. Introduction

Thiazole derivatives have attracted the attention of the scientific community in general and pharmaceutical chemists in particular (Potewar et al., 2007; Rajanarendar et al., 2012). This interest is largely fueled by the thiazole diverse pharmacological and biological activities. Many thiazoles are well-known anti-inflammatory, antimicrobial, antibacterial, analgesic, antihypertensive, herbicidal and/or anti-HIV agents (Abdel-Wahab et al., 2008; Gomha and Khalil, 2012; Verma and Saraf, 2008). The thiazole ring system represents the active handle in many biologically-active heterocyclic compounds (Abdel-Wahab et al., 2008; Abdelhamid et al., 2015; Dawood and Gomha, 2015; Gomha et al., 2015; Gomha et al., 2015b; Gomha and Khalil, 2012; Potewar et al., 2007; Rajanarendar et al., 2012; Sayed et al., 2020; Verma and

Saraf, 2008). Various thiazoles are biologically active scaffolds (Verma and Saraf, 2008), making them perfect candidates for library screening in medicinal chemistry (Oka et al., 2012; Watanabe and Uesugi, 2013). Many *bis*-thiazoles are also as reactive as their thiazole counterparts and their biological activity as antibacterial, antifungal, and anticancer were reported (Auterhoff, 1972; Franklin et al., 2008; Kouatly et al., 2009; Limban et al., 2012, 2011, 2008; Olar et al., 2010). In this study, our main focus is to construct some novel *bis*-thiazoles with high bioactivity profile. Accordingly, the starting carbazone is tagged with a hydroxyl group, which could be further functionalized as needed (Ou et al., 2013). This –OH handle could potentially be used to fine-tune structure–activity relationship (SAR). Herein, we introduce the preparation strategy of novel *bis*-thiazoles **6a-g** and **12a-c** as well as *bis*-thiazolone derivatives **9a-e** from synthetically simple *bis*-thiosemicarbazone derivative **3**, tagged with a hydroxyl group, with various hydrazonoyl chlorides **4a-g,** α-haloketones **10a-c**, and hydrazonoyl chlorides **4a-g** under basic reaction conditions. All new *bis*-heterocycles were structurally elucidated by elemental and spectral (^{1}H NMR, ^{13}C NMR, IR, and MS) analysis techniques. Furthermore, the biological profiles of the new bis-heterocycles were evaluated and the results were followed by *in-silico* docking studies and DFT calculations. Some of the new *bis*-thiazoles were good candidates as antimicrobial prototypes and could be further developed to target drug-resistant bacteria.

2. Results and discussion

2.1. Reaction chemistry

To kick-start our synthetic strategy, the common bis-thiosemicarbazone precursor **3** was constructed when one equivalent of hydroxyl-tagged bis-aldehyde **1** was condensed with two equivalents of thiosemicarbazide **2** in refluxing ethanol, acidified with HCl, for 2 h to give the new hydroxyl-bearing bis-thiosemicarbazone **3** as depicted in Scheme 1. The bis-aldehyde **1** itself was synthesized via reacting two equivalents of salicylaldehyde with epichlorohydrin in NaOH solution as previously reported by Bin, et al. (Zhao et al., 1996) (Scheme 1).

The chemical reactivity of the new hydroxyl-bearing bis-thiosemicarbazone **3** towards a host of hydrazonoyl chlorides **4** was evaluated to construct a new group of bis-thiazoles. Therefore, reaction of bis-thiosemicarbazone **3** with hydrazonoyl chlorides **4a-g** in refluxing dioxane in the presence of catalytic triethylamine delivered the target *bis*-thiazoles **6a-g** (Scheme 2). Elucidation of all the new *bis*-thiazole derivatives was executed using various spectral analyses. For example, the IR spectrum of compound **6f** revealed typical –NH absorption at the expected wave number ν 3410 cm^{-1}. Also, ^{1}H NMR spectrum of **6f** revealed four typical singlets for CH_3, CH-*OH*, *CH* = N, and *NH* groups at δ 2.60, 5.36, 8.51, and 11.36 ppm, respectively. The characteristic multiplet for the two CH_2 groups is visible at δ 4.19–4.25 ppm, in addition to the C-H multiplet shown at δ 5.40–5.45 ppm.

In a similar route, hydroxyl-tagged bis-thiosemicarbazone **3** reacted with *N*-aryl-2-oxopropanehydrazonoyl halides **7a-e** (the ester counterparts of compounds **4a-e**) in refluxing dioxane and catalytic triethylamine, leading to the formation of the expected bis-thiazole derivatives **9a-e** (Scheme 3). Elucidation of the new bis-heterocycles **9a-e** was substantiated typically by extensive spectral analysis. For example, the IR spectrum of derivative **9c** showed the presence of –NH absorption at 3396 and 3281 cm^{-1}characteristic for the four –NH groups. Further structural confirmation of the isolated bis-thiazole derivatives **9a-e** was based on their ^{1}H NMR spectra which contained four singlets for the CH-*OH*, *CH* = N and *2NH* groups near δ 5.36, 8.50, 9.42, and 11.37 ppm, respectively.

In a similar fashion, the reaction of compound **3** with phenacyl bromides **10a-c** in dioxane under reflux using catalytic triethylamine, afforded *bis*-thiazoles **12a-c** (Scheme 4). Structural analysis of the new *bis*-thiazoles was established using both spectral and elemental analyses. For example, the IR spectrum of product **12c** revealed –NH absorption at 3412 cm^{-1}. Moreover, the ^{1}H NMR spectra of the isolated compounds **12a-c** showed the characteristic four singlets at δ 3.78, 5.59, 8.93, and 11.35 ppm due to $2OCH_3$, CH-*OH*, thiazole-*CH* and 2*NH,* respectively. Also, two multiplets were shown at δ4.21–4.24 and 6.43–6.45 corresponding to the $2CH_2$ and the *CH*-OH groups, respectivly.

2.2. Molecular geometries

The molecular geometries of the studied compounds were subjected to energy minimization by implementing the B3LYP/6-311G level of theory. The obtained optimized structures and their corresponding frontier molecular orbitals (FMOs) are illustrated in Fig. 1. The calculated total energies are −83,764.15, −221,680.97, −83,579.12, −108,592.06 and −213,585.72 eV for **6c**, **6f, 9b, 9d,** and **12c**, respectively. Based on their relative energy values, compounds stability follows the

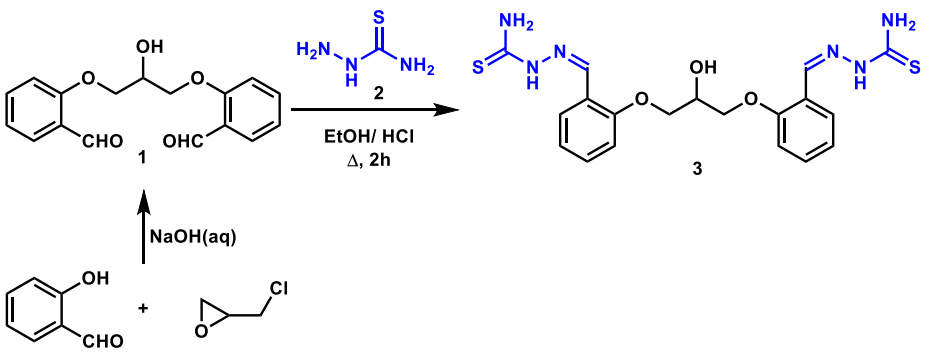

Scheme 1 Synthesis of bis-thiosemicarbazone**3.**

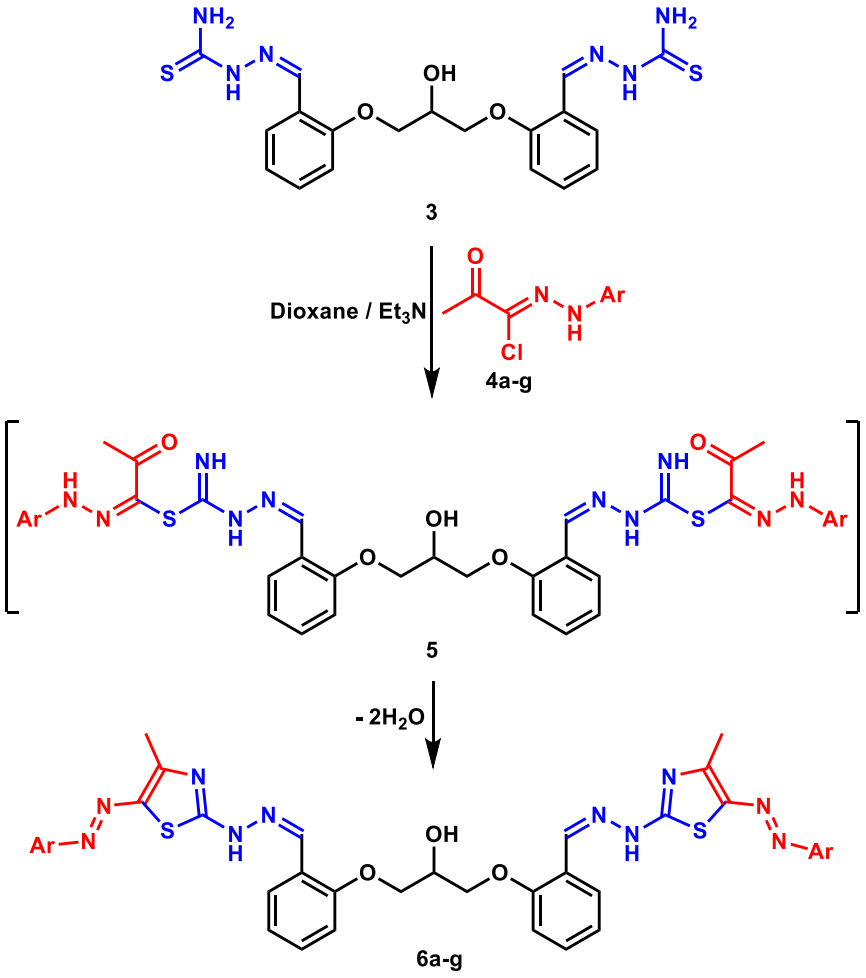

Ar = **a**, C_6H_5; **b**, 4-CH_3-C_6H_4; **c**, 4-Cl-C_6H_4; **d**, 4-NO_2-C_6H_4 **e**, 4-Br-C_6H_4; **f**, 2,4-Cl-C_6H_3; **g**, 2,4,6-Br-C_6H_2

Scheme 2 Synthesis of bis-thiazolesderivatives **6a-g.**

following order: **6f > 12c > 9d > 6c > 9b**. The quantum mechanical descriptors of the investigated molecules are collected in Table 1.

From the DFT energy calculations, some quantum chemical descriptors (Table 1) can be obtained that give information about the reactivity, complex formation with transition metals, the ability to donate/accept electrons, *etc*. For instance, ionization energy (I) and electron affinity (A) are two properties that can indicate the reactivity of the molecules. They can be calculated as follows: $I = -E_{HOMO}$ and $A = -E_{LUMO}$ (Abo Dena et al., 2019). Moreover, the complexation with transition metals requires having information about the softness (S) and/or hardness (η) of the molecules. Hardness is calculated from $\eta = (I - A)/2$ and softness is calculated as the reciprocal of hardness. Furthermore, during charge-transfer reactions, chemical potential ($\mu = -(I + A)/2$), Mullikan electronegativity ($\chi = (I + A)/2$) and electrophilicity index ($\omega = \mu^2/2\eta$) measure the lowering in energy that result from the maximal electron flow from the donor molecule to the acceptor molecule (Abo Dena and Abdel Gaber, 2017; Abo Dena and Hassan, 2016; Hassan and Abo Dena, 2014).

In order to make it easier to predict the chemical behavior/reactivity of the investigated organic molecules, the electrostatic potential maps (EPMs) were visualized (Fig. 2). In EPMs, areas of low electrostatic potential energy are shown in red color (nucleophilic sites), while blue areas indicate parts of low electron density (electrophilic sites). The compounds of interest contain areas susceptible for electrophilic addition, for instance the N atom of the thiazole rings and the OH groups. These are considered as electron-rich areas due to the localization of electron lone pairs on nitrogen and oxygen atoms. On the other hand, common functional groups or molecular parts that act as suitable sites for nucleophilic attack are represented by all aromatic and/or aliphatic hydrogens due to the strong electron attraction by the attached aromatic groups.

Interestingly, Frontier molecular orbitals are not only used for calculating the above-mentioned quantum mechanical descriptors, but also they can give information about light excitability and electron transfer through the molecules. HOMO refers to the highest occupied molecular orbital, while LUMO is an abbreviation for the lowest unoccupied molecular orbital. It is clear from the data illustrated in Table 1 that compound **6f** ($\Delta E = 2.94$ eV) has the highest light excitability as well as the highest heterogeneous electronic charge transfer among all of the investigated candidate compounds. Meanwhile, compound **12c** ($\Delta E = 3.9$) demonstrates the lowest light

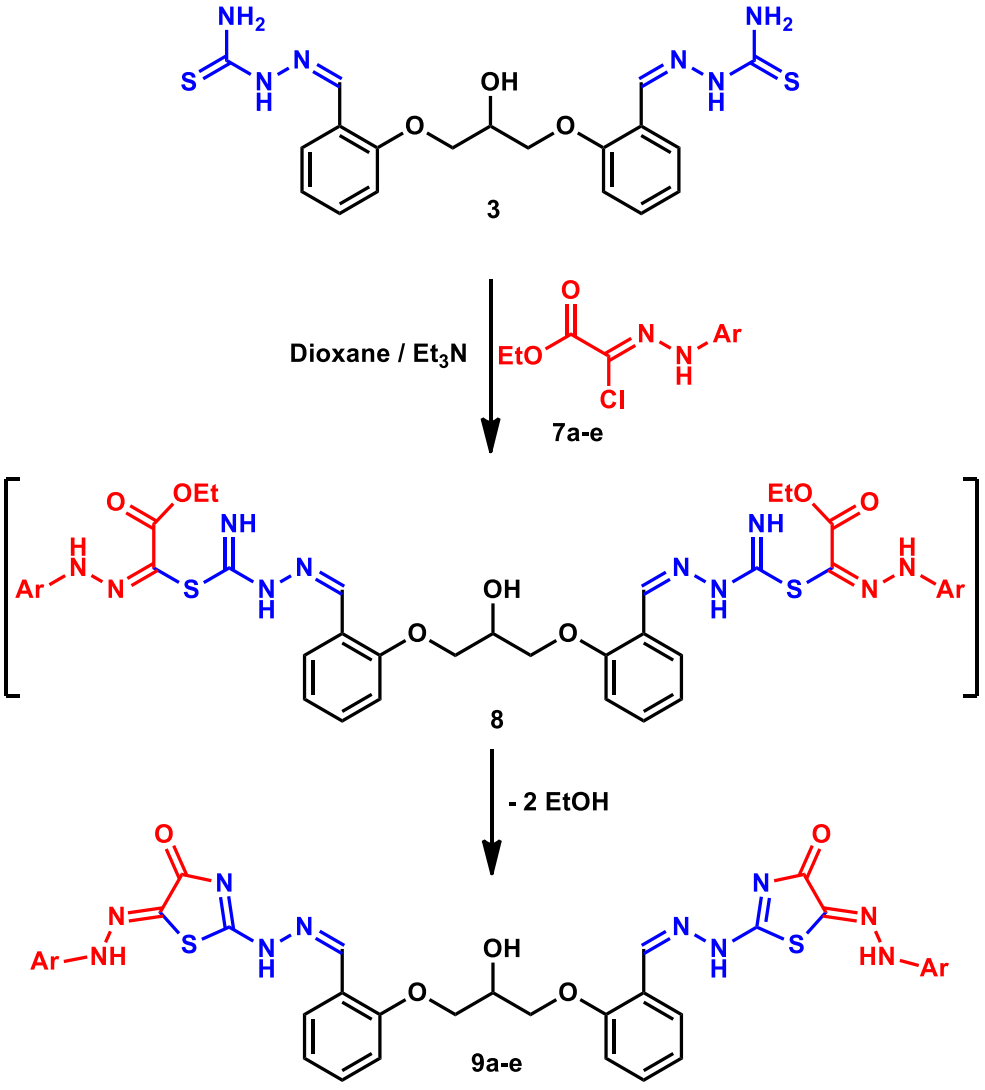

Scheme 3 Synthesis of bis-thiazole derivatives **9a-e.**

excitability and the lowest ability to catalyze heterogeneous electronic charge transfer. Due to the bilateral symmetry of the molecules, HOMOs are always delocalized in an opposite side to LUMOs of the same molecule. According to the above-mentioned ΔE values, it is expected that compound **12c** will absorb higher light energy (i.e. shorter wavelength) than compound **6f**.

2.3. XTT assay results

The cell proliferation kit II (XTT) assay was performed to find the minimum amounts (a.k.a. minimum inhibitory concentration, MIC) of the compounds that inhibit cell viability/metabolism of *P. aeruginosa*, *S. aureus* and *C. albicans*. The results obtained from the XTT assay are summarized in Table 2. Obviously, compound **9b** has excellent antibacterial (*P. aeruginosa*, MIC: 0.12 – 1.95 μg/mL) and antifungal (*C. albicans*, MIC: 0.98 – 3.90 μg/mL) activities, as reflected by the MIC values, compared to the standard antibiotic molecules, vancomycin, amikacin, and amphotericin B. In addition, molecule **12c** demonstrated an acceptable antibacterial activity against *S. aureus* (MIC: 0.98 – 1.95 μg/mL).

Table 2 showed that:

- Most of the studied molecules demonstrated greater antimicrobial activities against bacteria than fungi.
- All molecules showed different degrees of biological activities towards antibiotic-resistant *Staphylococcus aureus* (MRSA) TCC BAA-1720. The activity of compound **9b** (0.49 μg/mL) was greater than the standard antibiotic (0.98 μg/mL); however, compounds **6c, 6f, 9d** and **12c** showed the same effect (1.95 μg/mL).

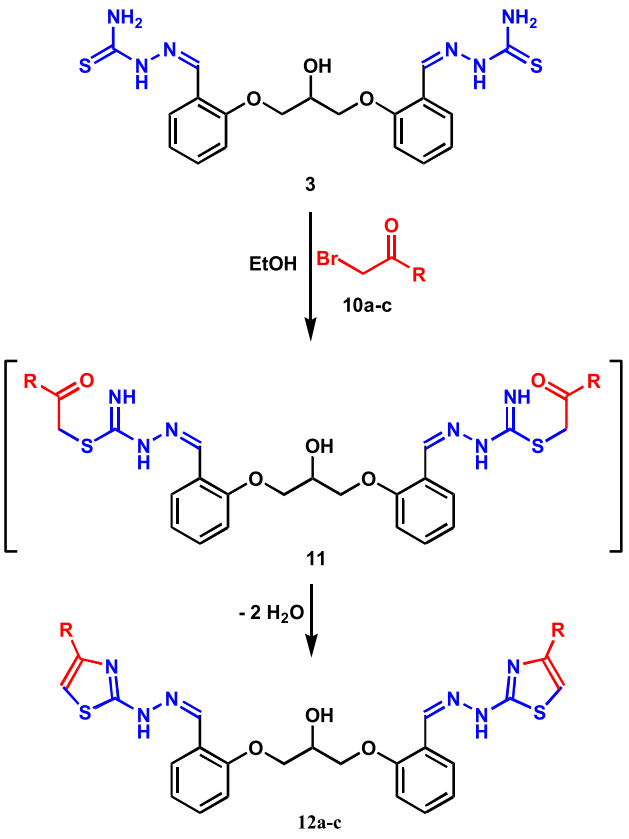

Scheme 4 Synthesis of bis-thiazole derivatives **12a-c.**

- The activity of compound **9b** against the antibiotic-sensitive *Pseudomonas aeruginosa* ATCC 10145 and the antibiotic-resistant *Pseudomonas aeruginosa* ATCC BAA-2108 was greater than that of vancomycin that showed an MIC value for the antibiotic-resistant strain similar to that of compound **9d**.
- On the other hand, all compounds did not have antimicrobial activity against Azole- resistant *Candida albicans* ATCC10231 fungus except compound **9b**.
- Compounds **9b** demonstrated a high antimicrobial effect against the antibiotic-resistant *P. aeruginosa* ATCC BAA-2108, and compound **9d** shows an acceptable antimicrobial activity in case of *P. aeruginosa* and *S. aureus* (MIC: 0.12 and 0.49 μg/mL, respectively).
- What's more, the antimicrobial activity of molecule **3** is very powerful as revealed from its very low MIC value. The compound was able to act against all resistant bacterial (*P. aeruginosa* and *S. aureus,* MIC: 0.49 and 3.9 μg/mL, respectively) and fungal (*C. albicans*, MIC: ND μg/mL) strains.
- Most of the synthesized molecules show very strong (MIC < 10 μg/mL) biological activity and few of them demonstrate either strong (MIC 10–25 μg/mL) or good (MIC 26–125 μg/mL) bioactivity according to the ranking reported elsewhere (O'Donnell et al., 2010).

2.4. Molecular docking

Molecular docking is a molecular modeling technique that helps in studying how two or more molecules fit together; for instance, a drug and an enzyme. It represents a potent tool in drug design and discovery of lead molecules. In the present study, this technique was applied to the investigated compounds to predict their biological activities. Reportedly, thiazoles and *bis*-thiazoles usually have powerful biological activities against *C. albicans* and *S. aureus*. Accordingly, those microorganisms were significantly influenced by treatment with the synthesized *bis*-thiazoles. The investigated compounds showed high toxicity to *Pseudomonas aeruginosa*. Consequently, we have chosen the most suitable microbial receptor proteins that can be influenced by *bis*-thiazole ligands based on a thorough literature review (Mahmoud et al., 2020).

Secreted Aspartic Proteinase (SAP) plays a significant role as an important virulence factor in *C. albicans* disseminated/-mucosal infections. The attachment/invasion of different *Candida* species, particularly *C. albicans*, is thought to be attributed to this protein, and hence it plays a crucial role in their pathogenicity. That is why SAPs can be a suitable target for drug intervention for candidiasis (Cutfield et al., 1995).

S. aureus is a common Gram-positive microbe which infects wounds resulting in increased incidence of staphylococcal scalded skin syndrome (a reaction of the skin to a staphylococcal exotoxin that can be absorbed into the blood stream) (Priyadarshi et al., 2010). Enoyl-[acyl-carrier-protein] reductase (FabI) is an enzyme of the FAS II system (a group of fatty acid synthases that catalyze fatty acids synthesis many types of bacteria and plants).

This enzyme is also crucial for other types of bacteria such as *Pseudomonas aeruginosa*. Accordingly, SAP and FabI were selected for with the studied molecules in order to relate the *in-silico* results with those of the experimental antibacterial tests.

Docking results indicated that the theoretical binding energies of the ligands are consistent with the experimental findings. For SAP (*C. albicans*), compound **9b** showed the best binding as indicated by the calculated energy of binding (-10.304 kcal/mol). However, compound **12c** demonstrated the highest binding energy (B.E., −8.736 kcal/mol) with the *S. aureus* protein, (FabI).

Finally, FabI receptor of *P. aeruginosa* shows the best affinity to compound **9b** with a calculated B.E. of −9.583 kcal/mol. It is worth mentioning that the arene-H dominated the types of receptor-ligand interactions in all of the above-mentioned cases, Fig. 3.

Clearly, the empirical MIC values of the investigated compounds are in good agreement with the theoretically computed binding energies. Consequently, compound **9b** may be suitable for inhibiting *C. albicans* and *P. aeruginosa* growth, while compound **12c** is suitable for retarding the growth of *S. aureus*.

3. Materials and methods

3.1. Synthesis and characterization

Melting points were determined on a Gallenkamp apparatus and are uncorrected. IR spectra were recorded via the KBr-

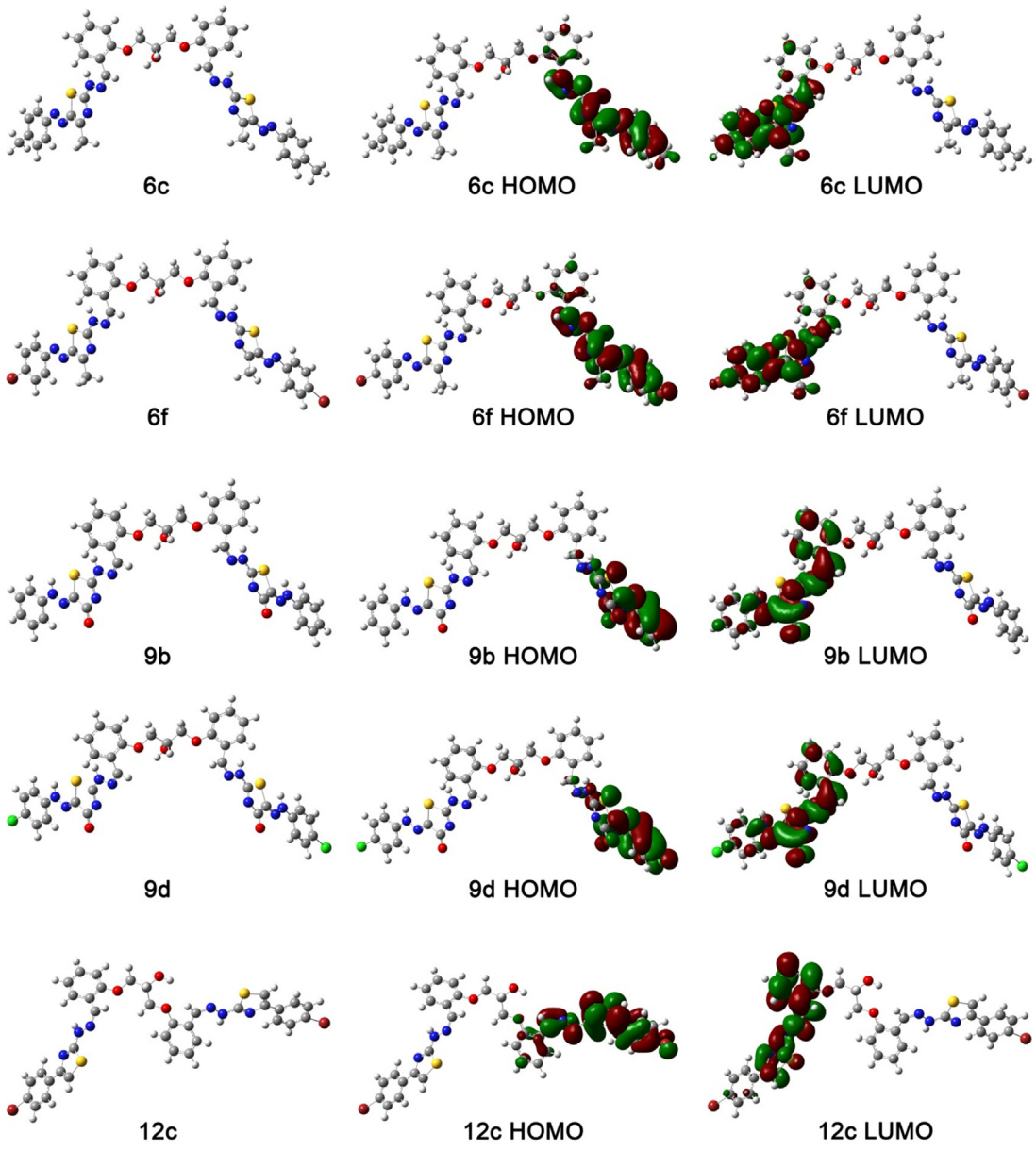

Fig. 1 Optimized molecular geometries of compounds **6c, 6f, 9b, 9d** and **12c** and their corresponding MOs. The isovalue used for visualization of the MOs is 0.02. Color codes: C: grey, O: red, H: white, N: blue, Cl: green, Br: brown, S: yellow.

disc method using a Pye-Unicam SP300 spectrophotometer. ^{1}H and ^{13}C NMR spectra were recorded in deuterated DMSO d_6 using a Varian Gemini 300 NMR spectrometer (300 MHz for ^{1}H NMR and 75 MHz for ^{13}C NMR) and the chemical shifts were related to that of the solvent DMSO d_6. Mass spectra were recorded with the aid of a GCMS-Q1000-EX Shimadzu and GCMS 5988-A HP spectrometers by applying an ionizing voltage of 70 eV. Elemental analyses were performed at the Microanalytical Centre, Faculty of Science, Cairo University, Giza, Egypt.

3.2. Synthesis of Bis-thiosemicarbazone derivative 3

A mixture of Hydroxy-*bis*-aldeyde**1**(3.0031 g, 0.01 mol), thiosemicarbazide(0.01 mol) and a few drops of conc. HCl in ethanol (30 mL) was refluxed for 3 h. The solid product which formed after cooling was collected and recrystallized from ethanol/dioxane as yellow crystals,72% yield; mp 229–230 °C; IR (KBr): *v* 3426 (OH), 3356,3252, 3147 (NH_2 and NH), 3062, 2986 (C-H) cm^{-1}; ^{1}H NMR (DMSO d_6):δ4.19–4.25 (m, 5H, 2CH_2, CH-OH), 5.39 (s, 1H, OH),6.96–6.98 (t, 2H, Ar-H), 7.10–7.12 (d, 2H, Ar-H), 7.35–7.39 (t, 2H, Ar-H), 7.92 (s, 2H, 2NH), 8.05–8.07 (d, 2H, Ar-H), 8.12 (s, 2H, 2NH), 8.50 (s, 2H, 2CH = N-), 11.37 (s, 2H, 2NH) ppm; ^{13}C NMR (DMSO d_6): δ68.2 (CH-OH), 69.7(CH_2O), 113.1, 121.2, 122.8, 126.5, 131.7, 139.0, 157.5 (Ar-C and N = C), 178.2 (C = S) ppm; MS *m*/*z* (%): 446 (M^+, 16), 435 (33), 410 (100), 373 (51), 320 (78), 299 (35), 210 (46), 126 (58), 60 (66)ppm; Anal. Calcd for $C_{19}H_{22}N_6O_3S_2$(446.54): C, 51.11; H, 4.97; N, 18.82. Found: C, 51.45; H, 4.65; N, 18.57%.

Table 1 Quantum chemical descriptors of the studied candidate molecules calculated by implementing the B3LYP/6-311G level of theory.

Quantum parameter	6c	6f	9b	9d	12c
Total energy (eV)	−83,764.15	−221,680.97	−83,579.12	−108,592.06	−213,585.72
E_{HOMO} (eV)	−5.47	−5.70	−5.89	−6.10	−5.82
E_{LUMO} (eV)	−2.48	−2.76	−2.43	−2.60	−1.92
ΔE (eV)	2.99	2.94	3.46	3.5	3.9
Ionization energy, I (eV)	5.47	5.70	5.89	6.10	5.82
Electron affinity, A (eV)	2.48	2.76	2.43	2.60	1.92
Mulliken electronegativity, χ	3.975	4.23	4.16	4.35	3.87
Chemical potential, μ (eV/mol)	−3.975	−4.23	−4.16	−4.35	−3.87
Softness, S	0.67	0.68	0.58	0.57	0.51
Hardness, η	1.50	1.47	1.73	1.75	1.95
Electrophilicity index, ω	5.28	6.09	5.00	5.41	3.84

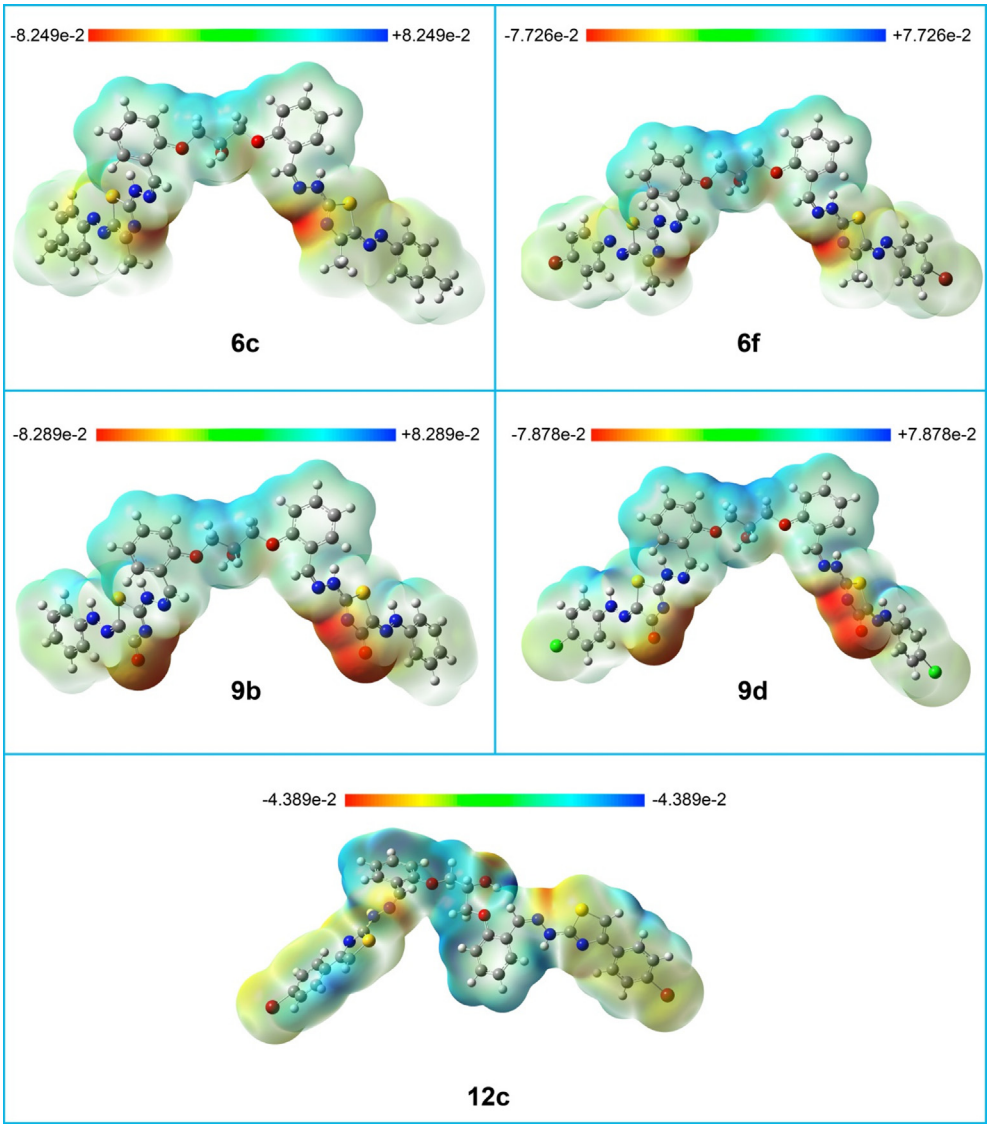

Fig. 2 Electrostatic potential maps of compounds **6c, 6f, 9b, 9d,** and **12c**. The isocalue of the electrostatic potntial ssurfaces is 0.0004.

Table 2 Antimicrobial activities in terms of MIC values of the investigated compounds against antibiotic-sensitive and antibiotic-resistant microorganisms as depicted from the XTT assay

Sample	Minimum inhibitory concentration (μg/mL)					
	Gram positive bacteria		Gram negative bacteria		Fungus	
	Methicillin-susceptible *Staphylococcus aureus* ATCC 25,923	Methicillin-resistant *Staphylococcus aureus (MRSA)* ATCC-BAA-1720	Sensitive *Pseudomonasaeruginosa* ATCC10145	Penicillin and Cephalosporins-resistant *Pseudomonas aeruginosa* ATCC BAA-2108	Azole-sensitive *Candida albicans* ATCC 18,804	Azole-Resistant *Candida albicans* ATCC 10,231
3	31.25	125	NA	NA	250	NA
6a	1.95	15.63	62.5	NA	125	NA
6b	7.81	31.25	31.25	NA	125	NA
6c	0.98	1.95	1.95	15.63	62.5	NA
6d	1.95	7.81	7.81	62.5	31.25	NA
6f	0.49	1.95	1.95	7.81	15.63	NA
6g	1.95	3.9	31.25	125	15.63	NA
9a	1.95	15.63	31.25	NA	NA	NA
9b	0.12	0.49	0.24	1.95	0.98	3.9
9c	0.98	3.9	3.9	7.81	3.9	15.63
9d	0.98	1.95	0.98	3.9	7.81	NA
9e	1.95	3.9	3.9	15.63	15.63	NA
12a	1.95	7.81	15.63	NA	62.5	NA
12b	7.81	15.63	15.63	NA	15.63	NA
12c	0.98	1.95	15.63	62.5	NA	NA
Vancomycin	0.24	0.98	0.49	3.9	ND	
Amikacin	0.98	7.81	0.24	3.9	ND	
Amphotericin B	ND	0.24	1.95			

3.2.1. Synthesis of bis-thiazole derivatives 6a-g, 9a-e and 12a-c

General procedure:To a stirred solution of thiosemicarbazone derivative **3**(1.0 g, 2.5 mmol) and hydrazonoyl chloride derivative **4a-g**, **7a-e**,orphenacyl bromide **10a-c** (2.5 mmol) in dioxane (30 mL), was added triethylamine (0.7 mL) and the mixture was refluxed for 5 h. The precipitated triethylamine hydrochloride was filtered off, and the solvent of the filtrate was subjected to evaporattion under reduced pressure. The residue was triturated with methanol. The formed solid was collected by filtration, washed with water, dried, and recrystallized from dioxane to afford the corresponding *bis*-thiazole derivatives **6a-g**,**9a-e** or **12a-c** respectively.

3.2.2. 1,3-Bis(2-((2-(4-methyl-5-(phenyldiazenyl)thiazol-2-yl) hydrazono)methyl)phenoxy)propan-2-ol (6a)

Red solid, 74% yield; mp. 190–191 °C; IR (KBr): *v* 3407 (2NH), 3037, 2933 (C-H) cm^{-1}; ^{1}H- NMR (DMSO d_6):δ 2.45 (s, 6H, $2CH_3$), 4.19–4.28 (m, 4H, $2CH_2$), 5.37 (s, 1H, OH), 5.70–5.71 (m, 1H, *CH*-OH), 6.96–7.92 (m, 18H, Ar-H), 8.50 (s, 2H, 2CH = N), 11.37 (s, 2H, 2NH) ppm; MS *m*/*z* (%): 731 (M^+, 30), 621 (47), 594 (44), 515 (36), 489 (100), 383 (23), 353 (31), 245 (54), 164 (16), 41 (65).Anal. Calcd for $C_{37}H_{34}N_{10}O_3S_2$(730.87): C, 60.81; H, 4.69; N, 19.16. Found: C, 60.53; H, 4.40; N, 18.85%.

3.2.3. 1,3-Bis(2-((2-(4-methyl-5-(p-tolyldiazenyl)thiazol-2-yl) hydrazono)methyl)phenoxy)propan-2-ol (6b)

Red solid, 71% yield; mp. 186–187 °C; IR (KBr): *v* 3410 (2NH), 3024, 2921 (C-H) cm^{-1}; ^{1}H- NMR (DMSO d_6):δ1.90 (s, 6H, $2CH_3$), 2.50 (s, 6H, $2CH_3$), 4.73–4.76 (m, 4H, $2CH_2$), 5.36 (m, 1H, *CH*-OH), 5.64 (s, 1H, OH), 7.03–8.05 (m, 16H, Ar-H), 8.12 (s, 2H, 2CH = N-), 10.41 (s, 2H, 2NH) ppm; ^{13}C-NMR (DMSO-d_6): δ 16.7, 18.9, 19.8, 22.5, 58.6, 65.4, 112.9, 114.1, 116.6, 120.7, 128.6, 129.9, 131.7, 132.5, 139.5, 143.9, 157.5 (Ar-H and C=N) ppm; MS *m*/*z* (%): 759 (M^+, 26), 716 (31), 670 (34), 617 (53), 596 (65), 510 (28), 480 (61), 407 (60), 380 (55), 313 (72), 289 (68), 226 (34), 179 (55), 102 (33), 43 (100).Anal. Calcd for $C_{39}H_{38}N_{10}O_3S_2$ (758.92): C, 61.72; H, 5.05; N, 18.46. Found: C, 61.50; H, 4.78; N, 18.28%.

3.2.4. 1,3-Bis(2-((2-(5-((4-chlorophenyl)diazenyl)-4-methylthiazol-2-yl)hydrazono)methyl) phenoxy)propan-2-ol (6c)

Red solid, 74% yield; mp. 151–152 °C; IR (KBr):*v* 3406 (2NH), 3098, 2927 (C-H) cm^{-1}; ^{1}H NMR (DMSO d_6):δ 2.57 (s, 6H, $2CH_3$), 4.21–4.26 (m, 4H, $2CH_2$), 5.40 (s, 1H, OH),5.69–5.70 (m, 1H, *CH*-OH), 6.94–7.53 (m, 16H, Ar-H), 8.50 (s, 2H, 2CH = N-), 10.66 (s, 2H, 2NH) ppm;MS *m*/*z* (%): 799 (M^+, 22), 720 (45), 687 (63), 608 (39), 545 (100), 480 (69), 325 (34), 207 (21), 167 (44), 149 (84), 135 (70), 44 (51). Anal. Calcd for $C_{37}H_{32}Cl_2N_{10}O_3S_2$ (799.75): C, 55.57; H, 4.03; N, 17.51. Found: C, 55.35; H, 3.75; N, 17.25%.

3.2.5. 1,3-Bis(2-((2-(4-methyl-5-((4-nitrophenyl)diazenyl) thiazol-2-yl)hydrazono)methyl)phenoxy) propan-2-ol (6d)

Red solid, 76% yield; mp. 169–170 °C; IR (KBr): *v* 3412, 333 (2NH), 3073, 2925 (CH) cm^{-1}; ^{1}H- NMR (DMSO d_6):δ 2.35 (s, 6H, $2CH_3$), 4.19–4.28 (m, 4H, $2CH_2$), 5.35 (s, 1H, OH),

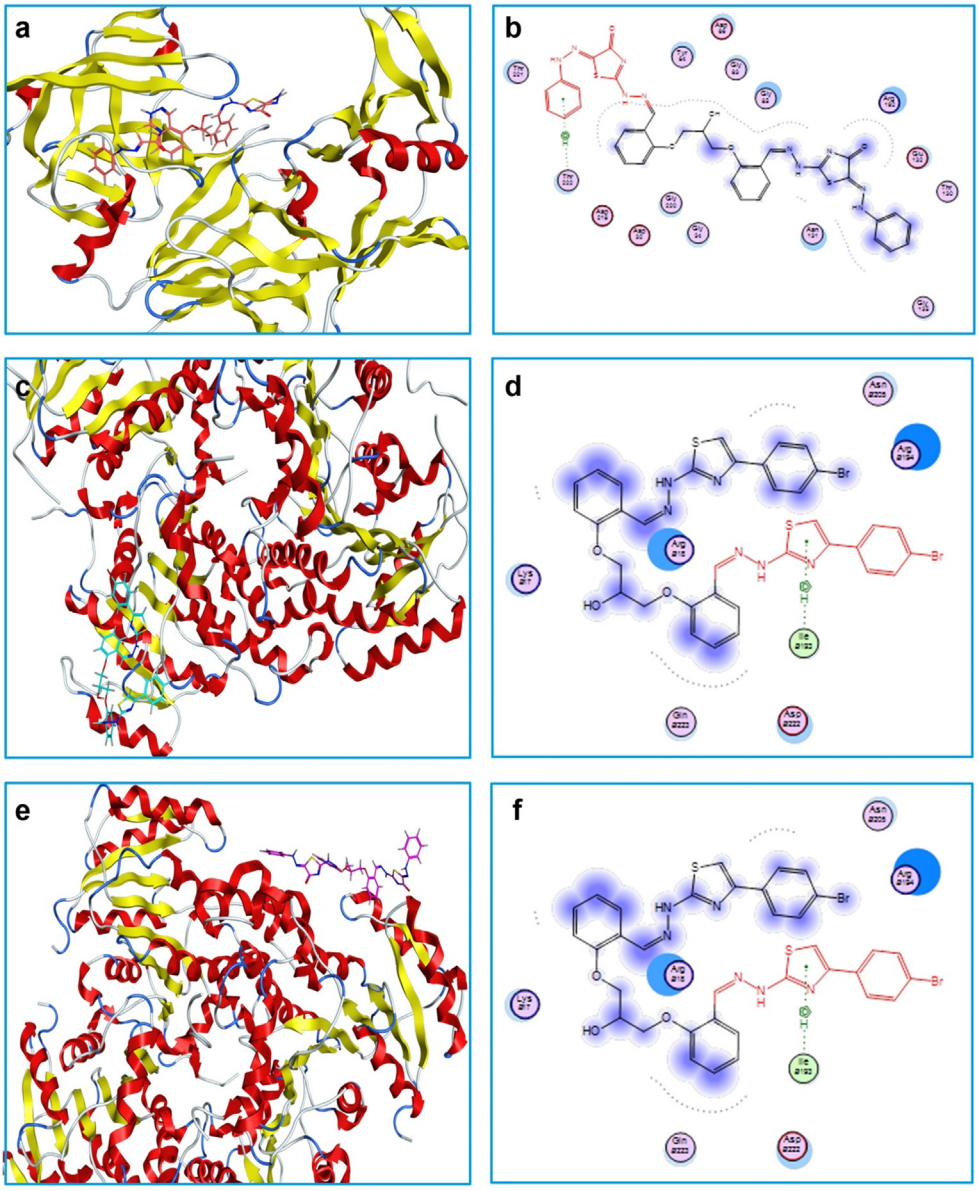

Fig. 3 Best receptor-ligand interaction poses (a, c and e) and ligand interaction diagrams (b, d and f) of compounds **9b** (with SAP of *C. albicans*), **12c** (with FabI of *S. aureus*) and **9b** (with FabI of *P. aeruginosa*), respectively.

5.68–5.70 (m, 1H, *CH*-OH), 7.01–8.12 (m, 16H, Ar-H), 8.95 (s, 2H, 2CH = N-), 11.36 (s, 2H, 2NH); MS *m/z* (%): 820 (M^+, 10), 792 (22), 671 (18), 595 (20), 460 (16), 358 (19), 291 (20), 181 (41), 91 (51), 66 (78), 45 (100).Anal. Calcd for $C_{37}H_{32}N_{12}O_7S_2$(820.86): C, 54.14; H, 3.93; N, 20.48. Found: C, 54.45; H, 3.65; N, 20.20 %.

3.2.6. 1,3-Bis(2-((2-(5-((4-bromophenyl)diazenyl)-4-methylthiazol-2-yl)hydrazono)methyl) phenoxy)propan-2-ol (6e)

Red solid, 78% yield; mp. 148–149 °C; IR (KBr): *v* 3418 (2NH), 3074, 2925 (CH) cm^{-1}; ^{1}H NMR (DMSO d_6):*δ* 2.56 (s, 6H, $2CH_3$), 4.03–4.33 (m, 5H, $2CH_2$, *CH*-OH), 5.62 (s, 1H, OH), 7.05–7.97 (m, 16H, Ar-H), 8.96 (s, 2H, 2CH = N-), 10.62 (s, 2H, 2NH); ^{13}C-NMR (DMSO-d_6): *δ* 18.9, 23.6, 63.2, 68.0, 116.5, 118.4, 120.1, 121.3, 122.4, 123.7, 125.6, 126.3, 128.1, 132.3, 139.1, 170.8 (Ar-H and C = N) ppm; MS *m/z* (%): 888 (M^+, 25), 785 (48), 659 (27), 508 (28), 413 (100), 303 (31), 258 (50), 182 (56), 126 (65), 104 (75), 62 (92).Anal. Calcd for $C_{37}H_{32}Br_2N_{10}O_3S_2$(888.66): C, 50.01; H, 3.63; N, 15.76. Found: C, 49.76; H, 3.45; N, 15.55%.

3.2.7. 1,3-Bis(2-((2-(5-((2,4-dichlorophenyl)diazenyl)-4-methylthiazol-2-yl)hydrazono)methyl) phenoxy)propan-2-ol (6f)

Red solid, 69% yield; mp. 180–181 °C; IR (KBr): *v* 3410 (2NH), 3300, 2929 (CH) cm^{-1}; ^{1}H NMR (DMSO d_6):*δ* 2.60 (s, 6H, $2CH_3$), 4.19–4.25 (m, 4H, $2CH_2$), 5.36 (s, 1H, OH), 5.40–5.42 (m, 1H, *CH*-OH), 6.94–8.12 (m, 14H, Ar-H), 8.51 (s, 2H, 2CH = N-), 11.36 (s, 2H, 2NH); MS *m/z* (%): 868 (M^+, 11), 852 (24), 816 (39), 763 (20), 728 (17), 658 (19), 567 (13), 422 (100), 386 (28), 243 (73), 148 (20), 85 (40).Anal.

Calcd for $C_{37}H_{30}Cl_4N_{10}O_3S_2$ (868.63): C, 51.16; H, 3.48; N, 16.13. Found: C, 51.53; H, 3.15; N, 15.89%.

3.2.8. 1,3-Bis(2-((2-(4-methyl-5-((2,4,6-tribromophenyl)diazenyl)thiazol-2-yl)hydrazono)methyl) phenoxy)propan-2-ol (6 g)

Red solid, 70% yield; mp. 163–164 °C; IR (KBr):*v* 3402 (2NH), 3175, 2923 (CH) cm^{-1}; ^1H NMR (DMSO d_6):δ 2.50 (s, 6H, $2CH_3$), 4.19–4.25 (m, 4H, $2CH_2$), 4.53 (s, 1H, OH), 5.65 (m, 1H, *CH*-OH), 6.94–8.13 (m, 12H, Ar-H), 8.50 (s, 2H, 2CH = N-), 11.36 (s, 2H, 2NH)ppm; ^{13}C-NMR (DMSO-d_6): δ 28.9, 32.1, 65.6, 89.5, 113.5, 116.6, 118.3, 120.9, 123.7, 125.5, 128.2, 129.9, 130.8, 34.3, 134.9, 147.9 (Ar-H and C=N) ppm; MS *m*/*z* (%): 1204 (M^+, 18), 994 (13), 891 (18), 730 (30), 693 (26), 660 (33), 545 (38), 478 (76), 406 (35), 368 (55), 341 (23), 204 (19), 176 (23), 116 (100), 96 (42).Anal. Calcd for $C_{37}H_{28}Br_6N_{10}O_3S_2$ (1204.24): C, 36.90; H, 2.34; N, 11.63. Found: C, 37.17; H, 2.11; N, 11.51 %.

3.2.9. 2,2′-(((((2-Hydroxypropane-1,3-diyl)bis(oxy))bis(2,1-phenylene))bis(methanylylidene)) bis(hydrazin-1-yl-2-ylidene))bis(5-(2-phenylhydrazono)thiazol-4(5H)-one) (9a)

Yellow solid, 76% yield; mp. 170–172 °C; IR (KBr): *v* 3396, 3281 (4NH), 3173, 3033, 2975 (CH), 1678 (2C = O) cm^{-1}; ^1H NMR (DMSO d_6):δ4.02–4.21 (m, 5H, $2CH_2$, *CH*-OH), 5.42 (s, 1H, OH), 7.01–7.92 (m, 18H, Ar-H), 8.82 (s, 2H, 2CH = N-), 10.81 (s, 2H, 2NH), 11.36 (s, 2H, 2NH) ppm; MS *m*/*z* (%): 734 (M^+, 35), 582 (48), 651 (16), 563 (34), 519 (14), 448 (100), 422 (68), 412 (31), 349 (39), 317 (22), 292 (20), 218 (26), 166 (57), 143 (39), 80 (38). Anal. Calcd for $C_{35}H_{30}N_{10}O_5S_2$ (734.81): C, 57.21; H, 4.12; N, 19.06. Found: C, 57.00; H, 3.94; N, 18.88 %.

3.2.10. 2,2′-(((((2-Hydroxypropane-1,3-diyl)bis(oxy))bis (2,1-phenylene))bis(methanylylidene))bis (hydrazin-1-yl-2-ylidene))bis(5-(2-(p-tolyl)hydrazono)thiazol-4(5H)-one) (9b)

Yellow solid, 73% yield; mp. 175–176 °C; IR (KBr): *v* 3403, 3286 (4NH), 3073, 2975 (CH), 1689 (2C = O) cm^{-1}; ^1H NMR (DMSO d_6):δ 2.42 (s, 6H, $2CH_3$), 4.05–4.35 (m, 4H, $2CH_2$, *CH*-OH), 5.40 (s, 1H, OH), 6.94–7.91 (m, 16H, Ar-H), 8.50 (s, 2H, 2CH = N-), 10.26 (s, 2H, 2NH), 11.36 (s, 2H, 2NH) ppm; ^{13}C-NMR (DMSO-d_6): δ 14.4, 28.8, 32.0, 61.9, 115.7, 116.5, 120.7, 122.4, 127.5, 129.6, 133.2, 137.9, 142.1, 143.1, 152.1 (Ar-H and C=N) , 162 (2C=O) ppm; MS *m*/*z* (%): 763 (M^+, 7), 737 (8), 639 (8), 562 (15), 509 (13), 412 (100), 385 (15), 216 (35), 164 (22), 120 (24), 91 (27), 61 (20). Anal. Calcd for $C_{37}H_{34}N_{10}O_5S_2$ (762.86): C, 58.26; H, 4.49; N, 18.36. Found: C, 58.55; H, 4.24; N, 18.14%.

3.2.11. 2,2′-(((((2-Hydroxypropane-1,3-diyl)bis(oxy))bis (2,1-phenylene))bis(methanylylidene))bis (hydrazin-1-yl-2-ylidene))bis(5-(2-(4-chlorophenyl)hydrazono)thiazol-4(5H)-one) (9c)

Yellow solid, 74% yield; mp. 200–201 °C; IR (KBr): *v* 3430, 3263 (4NH), 3157, 2978 (CH), 1707 (C = O) cm^{-1}; ^1H NMR (DMSO d_6):δ4.03–4.24 (m, 5H, $2CH_2$, *CH*-OH), 5.36 (s, 1H, OH), 6.94–8.14 (m, 16H, Ar-H), 8.50 (s, 2H, 2CH = N-), 10.64 (s, 2H, 2NH), 11.36 (s, 2H, 2NH) ppm; ^{13}C-NMR (DMSO-d_6): δ 63.2, 67.9, 69.6, 113.0, 121.2, 122.8, 125.3, 126.5, 129.5, 130.2, 131.8, 139.0, 157.5, 163.5 (Ar-H and C=N), 178.1 (2C=O) ppm; MS *m*/*z* (%): 803 (M^+, 7), 764 (8), 667 (6), 602 (13), 544 (3), 421 (10), 333 (95), 318 (64), 251 (53), 214 (28), 173 (36), 147 (69), 118 (58), 91 (48), 65 (100).Anal. Calcd for $C_{35}H_{28}Cl_2N_{10}O_5S_2$ (803.69): C, 52.31; H, 3.51; N, 17.43. Found: C, 52.55; H, 3.30; N, 17.16%.

3.2.12. 2,2′-(((((2-Hydroxypropane-1,3-diyl)bis(oxy))bis (2,1-phenylene))bis(methanylylidene))bis (hydrazin-1-yl-2-ylidene))bis(5-(2-(4-nitrophenyl)hydrazono)thiazol-4(5H)-one) (9d)

Yellow solid, 70% yield; mp. 190–192 °C; IR (KBr):*v* 3446, 3204 (4NH), 3058, 2947 (C-H), 1708 (C = O) cm^{-1}; ^1H NMR (DMSO d_6):δ 2.22 (s, 6H, $2CH_3$), 4.17–4.28 (m, 5H, $2CH_2$, *CH*-OH), 5.64 (s, 1H, OH), 6.94–8.06 (m, 16H, Ar-H), 8.80 (s, 2H, 2CH = N-), 10.54 (s, 2H, 2NH), 11.35 (s, 2H, 2NH) ppm; MS *m*/*z* (%): 825 (M^+, 60), 737 (35), 707 (25), 650 (29), 551 (48), 513 (30), 474 (61), 388 (31), 341 (35), 268 (30), 214 (32), 199 (23), 75 (88), 57 (100). Anal. Calcd for $C_{35}H_{28}N_{12}O_9S_2$(824.80): C, 50.97; H, 3.42; N, 20.38;. Found: C, 51.19; H, 3.19; N, 20.17%.

3.2.13. 2,2′-(((((2-Hydroxypropane-1,3-diyl)bis(oxy))bis (2,1-phenylene))bis(methanylylidene))bis (hydrazin-1-yl-2-ylidene))bis(5-(2-(2,4-dichlorophenyl)hydrazono)thiazol-4 (5H)-one) (9e)

Yellow solid, 73% yield; mp. 188–189 °C; IR (KBr): *v* 3425, 3264 (4NH), 3154, 2974 (CH), 1716 (2C = O) cm^{-1}; ^1H NMR (DMSO d_6):δ4.22–4.25 (m, 5H, $2CH_2$, *CH*-OH), 5.37 (s, 1H, OH), 6.94–8.12 (m, 14H, Ar-H), 8.50 (s, 2H, 2CH = N-), 9.42 (s, 2H, 2NH), 11.37 (s, 2H, 2NH) ppm: MS *m*/*z* (%): 872 (M^+, 26), 828 (92), 763 (22), 752 (35), 678 (26), 608 (37), 576 (16), 431 (23), 310 (100), 280 (70), 138 (62), 111 (53), 77 (50) . Anal. Calcd for $C_{35}H_{26}Cl_4N_{10}O_5S_2$(872.58): C, 48.18; H, 3.00; N, 16.05. Found: C, 48.36; H, 2.84; N, 15.85%.

3.2.14. 1,3-Bis(2-((2-(4-(4-chlorophenyl)thiazol-2-yl) hydrazono)methyl)phenoxy)propan-2-ol (12a)

Brown solid, 70% yield; mp. 255–256 °C; IR (KBr): *v* 3412 (2NH), 3062, 2928 (CH) cm^{-1}; ^1H- NMR (DMSO d_6):δ4.25–4.29 (m, 5H, $2CH_2$, *CH*-OH), 5.70 (s, 1H, OH), 7.28 (s, 2H, 2CH-thiazole-H), 7.55–8.36 (m, 16H, Ar-H), 8.79 (s, 2H, 2CH = N-), 10.44 (s, 2H, 2NH) ppm; ^{13}C-NMR (DMSO-d_6): δ 55.7, 56.2, 114.2, 115.1, 117.9, 119.4, 121.3, 122.3, 125.0, 130.6, 132.4, 136.8, 160.4, 165.1, 166.9 (Ar-H and C=N) ppm; MS *m*/*z* (%): 715 (M^+, 31), 696 (18), 615 (22), 573 (43), 500 (39), 480 (44), 422 (49), 396 (32), 360 (31), 210 (100), 171 (37), 143 (20), 117 (42). Anal. Calcd for $C_{35}H_{28}Cl_2N_6O_3S_2$(715.67): C, 58.74; H, 3.94; N, 11.74. Found: C, 59.00; H, 3.72; N, 11.52%.

3.2.15. 1,3-Bis(2-((2-(4-(4-bromophenyl)thiazol-2-yl) hydrazono)methyl)phenoxy)propan-2-ol (12b)

Brown solid, 76% yield; mp. 250–251 °C; IR (KBr): *v* 3387 (2NH), 3063, 2926 (CH) cm^{-1}; ^1H- NMR (DMSO d_6):δ 2.58 (s, 6H, $2CH_3$), 4.12–4.22 (m, 5H, $2CH_2$, *CH*-OH), 5.65 (s, 1H, OH), 7.27 (s, 2H, 2CH-thiazole-H), 7.47–8.21 (m, 16H, Ar-H), 8.40 (s, 2H, 2CH = N-), 11.96 (s, 2H, 2NH) ppm; ^{13}C-NMR (DMSO-d_6): δ 32.8, 34.8, 66.8, 114.7, 118.2, 121.4,

128.7, 130.9, 131.1, 132.6, 133.8, 144.8, 153.3, 161.0, 162.6 (Ar-H and C = N) ppm; MS *m/z* (%): 804 (M^+, 16), 774 (27), 741 (37), 663 (22), 607 (28), 575 (23), 512 (41), 483 (40), 465 (63), 348 (74), 283 (30), 186 (100), 166 (58), 102 (46), 75 (35). Anal. Calcd for $C_{35}H_{28}Br_2N_6O_3S_2$(804.58): C, 52.25; H, 3.51; N, 10.45. Found: C, 52.51; H, 3.33; N, 10.19%.

3.2.16. 1,3-Bis(2-((2-(4-(4-methoxyphenyl)thiazol-2-yl) hydrazono)methyl)phenoxy)propan-2-ol (12c)

Brown solid, 65% yield; mp. 269–270 °C; IR (KBr):*v* 3403 (2NH), 3068, 2936 (CH) cm^{-1}; ^1H NMR (DMSO d_6):δ 3.78 (s, 6H, $2OCH_3$), 4.21–4.24 (m, 5H, $2CH_2$, *CH*-OH), 5.59 (s, 1H, OH), 6.43–8.06 (m, 16H, Ar-H), 8.93 (s, 2H, 2CH-thiazole-H), 8.48 (s, 2H, 2CH = N-), 11.35 (s, 2H, 2NH) ppm; MS *m/z* (%): 706 (M^+, 26), 688 (30), 642 (25), 576 (19), 512 (22), 480 (33), 422 (35), 355 (100), 313 (27), 239 (22), 151 (39), 101 (42). Anal. Calcd for $C_{37}H_{34}N_6O_5S_2$(706.84): C, 62.87; H, 4.85; N, 11.89. Found: C, 63.20; H, 4.59; N, 11.61%.

3.3. In-vitro XTT assay

XTT assay (Al-Bakri and Afifi, 2007; Kuhn et al., 2003; Liang et al., 2012; Monteiro et al., 2012) is a non-radioactive spectrophotometric assay usually used for measuring cell viability and proliferation via the assessment of the cellular metabolic activity. The assay depends on the chemical reduction of the XTT dye (a yellow tetrazolium salt) to an orange formazan dye by living cells. The minimal inhibitory concentration values represent the lowest concentrations of test or standard drugs (vancomycin and amikacin for bacteria, and amphotericin B for fungi) that completely inhibit microbial growth. For determining the MIC values, the microdilution method was applied. Briefly, the microbial inoculum was prepared and the concentrations of the suspensions were adjusted to 10^6 CFU/mL. Solutions of the standard and test molecules were prepared in dimethyl sulfoxide (DMSO) and subsequent two-fold dilutions were carried out in a 96-well microplate. Each well of the microplate included 40 µL of the Brain Heart Infusion (BHI) growth medium, 10 µL of the microbial inoculum and 50 µL of the investigated molecules diluted to final concentrations of 1000–0.12 µg/mL. Pure DMSO was used as a blank. The plates were incubated for 24 h at 37 °C; thereafter, 40 µL of XTT tetrazolium salt were added. Consequently, the plates were incubated at 37 °C in a dark environment for 1 h, and then the color change was measured spectrophotometrically at 492 nm using a microtiterplate reader (Tecan Sunrise absorbance reader; Tecan UK, Reading, United Kingdom). MIC values were determined as the minimum concentrations that caused the largest color change compared to the blank.

3.4. Theoretical calculations

Geomtery optimizations were implemented, using DFT algorithms at the B3LYP/6-311G level of theory, with the aid of Gaussian 09 W package (Gomha et al., 2016a). The obtained molecular geometries and their corresponding molecular orbitals were visualized using GaussView 5.0.9 package. Becke's three-parameter hybrid method (B3LYP) demonstrates more accurate results than the pure Hartree-Fock method (Gomha et al., 2016b). B3LYP represents the combinaton of the correlation functional of Lee, Yang and Parr with Becke's three parameters (Lee et al., 1988).

Table 3 Protein receptors applied in the molecular docking studies.

PDB ID	Receptor name	Resolution	Organism
1EAG	Secreted aspartic proteinase (SAP2) from *Candida albicans*complexed with A70450	X-Ray Diffraction, 2.1 Å	*Candida albicans*
3GR6	Crystal structure of the *Staphylococcus aureus*enoyl-acyl carrier protein reductase (FabI) in complex with NADP and triclosan	X-Ray Diffraction, 2.28 Å	*Staphylococcus aureus*
4NR0	Crystal structure of the *Pseudomonas aeruginosa*enoyl-acyl carrier protein reductase (FabI) in complex with NAD + and triclosan	X-Ray Diffraction, 1.779 Å	*Pseudomonas aeruginosa*

3.5. Molecular docking

Molecular docking was performed using Molecular Operating Environment (MOE) 2014 software (Group, 2014). Compounds that showed the lowest MIC values in the XTT assay were selected and docked with the corresponding target proteins. The compounds were subjected to energy minimzation using the MMFF94x force field prior to docking. High resolution 3D molecular structures of the receptors (Table 3) were obtained from the Protein Data Bank (PDB).

4. Conclusions

Finally, we succeeded to synthesize novel carbazones as precursors for the preparation of a novel series of *bis*-thiazole and *bis*-thiazolone derivatives. The mechanistic pathways and the chemical structures of all synthesized derivatives were explained and confirmed relying on the available spectral data. The antimicrobial activity results of the tested *bis*-thiazole and *bis*-thiazolone showed that some derivatives have moderate to no activity against the tested fungal and bacterial strains. Only one derivative (**9b),** being the most active against all bacteria and fungi, was equipotent to the standard antibiotic, vancomycin. Molecular docking simulations of the prepared compounds revealed the activity of compouns **9b** (with SAP of *C. albicans*), **12c** (with FabI of *S. aureus*) and **9b** (with FabI of *P. aeruginosa*), respectively. DFT calculations were employed to obtain information about geometries, chemical reactivity and optical/electronic properties of the synthesized compounds. The candidate molecules are promising antimicrobial agents and can be used as lead compounds for the preparation of novel antibiotics for antibiotic-resistant bacterial species.

Author contributions

S.M.G. and R. M. K. conceived the experiment(s); S.M.G., R. M.K., A.S.A.D., M.M.A., S.A.A., M.E.Z and Z.A.M. conducted the experiment(s); S.M.G., R. M. K. and Z.A.M. analyzed the results. All authors reviewed the manuscript.

Declaration of Competing Interest

The authors declare that they have no known competing financial interests or personal relationships that could have appeared to influence the work reported in this paper.

Acknowledgment

The authors extend their appreciation to the Deanship of Scientific Research at Imam Mohammad Ibn Saud Islamic University for funding this work through Research Group no-RG. 21-09-76.

Appendix A. Supplementary data

Supplementary data to this article can be found online at https://doi.org/10.1016/j.arabjc.2021.103396.

References

Abdel-Wahab, B.F., Mohamed, S.F., Amr, A.-G., Abdalla, M.M., 2008. Synthesis and reactions of thiosemicarbazides, triazoles, and Schiff bases as antihypertensive α-blocking agents. Monatshefte für Chemie - Chem. Mon. 139 (9), 1083–1090. https://doi.org/10.1007/s00706-008-0896-2.

Abdelhamid, A.O., Shawali, A.S., Gomha, S.S., El-Enany, W.A.M.A., 2015. Synthesis and Antimicrobial Evaluation of Some Novel Thiazole, 1,3,4-Thiadiazole and Pyrido[2,3-d][1,2,4]triazolo[4,3-a] pyrimidine Derivatives Incorporating Pyrazole Moiety. Heterocycles 91, 2126–2142. https://doi.org/10.3987/COM-15-13319.

Abo Dena, A.S., Abdel Gaber, S.A., 2017. In vitro drug interaction of levocetirizine and diclofenac: Theoretical and spectroscopic studies. Spectrochim. Acta - Part A Mol. Biomol. Spectrosc. 181, 239–248. https://doi.org/10.1016/j.saa.2017.03.043.

Abo Dena, A.S., Hassan, W.M.I., 2016. Experimental and quantum mechanical studies on the ion–pair of levocetirizine and bromocresol green in aqueous solutions. Spectrochim. Acta Part A Mol. Biomol. Spectrosc. 163, 108–114. https://doi.org/10.1016/j.saa.2016.03.030.

Abo Dena, A.S., Muhammad, Z.A., Hassan, W.M.I., 2019. Spectroscopic, DFT studies and electronic properties of novel functionalized bis-1,3,4-thiadiazoles. Chem. Pap. https://doi.org/10.1007/s11696-019-00833-7

Al-Bakri, A.G., Afifi, F.U., 2007. Evaluation of antimicrobial activity of selected plant extracts by rapid XTT colorimetry and bacterial enumeration. J. Microbiol. Methods 68 (1), 19–25. https://doi.org/10.1016/j.mimet.2006.05.013.

Auterhoff, H., 1972. Textbook of Organic Medicinal and Pharmaceutical Chemistry. Herausgegeben von Ch.O. Wilson, O. Gisvold und R.G. Doerge. 6. Auflage, 1053 Seiten. J.B. Lippincott Co, Philadelphia and Toronto, und Blackwell Scientific Publications, Oxford and Edinburgh 1971. Arch. Pharm. (Weinheim). 305, 316. https://doi.org/10.1002/ardp.19723050418

Cutfield, S.M., Dodson, E.J., Anderson, B.F., Moody, PCE, Marshall, C.J., Sullivan, P.A., Cutfield, J.F., 1995. The crystal structure of a major secreted aspartic proteinase from Candida albicans in complexes with two inhibitors. Structure 3 (11), 1261–1271.

Dawood, K.M., Gomha, S.M., 2015. Synthesis and Anti-cancer Activity of 1,3,4-Thiadiazole and 1,3-Thiazole Derivatives Having 1,3,4-Oxadiazole Moiety. J. Heterocycl. Chem. 52, 1400–1405. https://doi.org/10.1002/jhet.2250.

Franklin, P.X., Pillai, A.D., Rathod, P.D., Yerande, S., Nivsarkar, M., Padh, H., Vasu, K.K., Sudarsanam, V., 2008. 2-Amino-5-thiazolyl motif: A novel scaffold for designing anti-inflammatory agents of diverse structures. Eur. J. Med. Chem. 43 (1), 129–134. https://doi.org/10.1016/j.ejmech.2007.02.008.

Gomha, S.M., Badrey, M.G., Edrees, M.M., 2016a. Heterocyclisation of 2,5-diacetyl-3,4-disubstituted-thieno[2,3-b]Thiophene Bis-Thiosemicarbazones Leading to Bis-Thiazoles and Bis-1,3,4-thiadiazoles as Anti-breast Cancer Agents. J. Chem. Res. 40 (2), 120–125. https://doi.org/10.3184/174751916X14537182696214.

Gomha, S., Edrees, M., Altalbawy, F., 2016b. Synthesis and Characterization of Some New Bis-Pyrazolyl-Thiazoles Incorporating the Thiophene Moiety as Potent Anti-Tumor Agents. Int. J. Mol. Sci. 17 (9), 1499. https://doi.org/10.3390/ijms17091499.

Gomha, S.M., Khalil, K., Abdel-Aziz, H., Abdalla, M., 2015a. Synthesis and Antihypertensive α-Blocking Activity Evaluation of Thiazole Derivatives Bearing Pyrazole Moiety. Heterocycles 91, 1763–1773. https://doi.org/10.3987/COM-15-13290.

Gomha, S.M., Khalil, K.D., 2012. A convenient ultrasound-promoted synthesis of some new thiazole derivatives bearing a coumarin nucleus and their cytotoxic activity. Molecules 17, 9335–9347. https://doi.org/10.3390/molecules17089335.

Gomha, S.M., Riyadh, S.M., Mahmmoud, E.A., Elaasser, M.M., 2015b. Synthesis and anticancer activity of arylazothiazoles and 1,3,4-thiadiazoles using chitosan-grafted-poly(4-vinylpyridine) as a novel copolymer basic catalyst. Chem. Heterocycl. Compd. 51 (11-12), 1030–1038. https://doi.org/10.1007/s10593-016-1815-9.

Group, C.C., 2014. Molecular Operating Environment.

Hassan, W.M.I., Abo Dena, A.S., 2014. Unraveling the nature of interaction between substituted phenol and amiodarone. Anal. Chem. 86 (3), 1881–1886. https://doi.org/10.1021/ac403964b.

Kouatly, O., Geronikaki, A., Kamoutsis, C., Hadjipavlou-Litina, D., Eleftheriou, P., 2009. Adamantane derivatives of thiazolyl-N-substituted amide, as possible non-steroidal anti-inflammatory agents. Eur. J. Med. Chem. 44 (3), 1198–1204. https://doi.org/10.1016/j.ejmech.2008.05.029.

Kuhn, D.M., Balkis, M., Chandra, J., Mukherjee, P.K., Ghannoum, M.A., 2003. Uses and limitations of the XTT assay in studies of Candida growth and metabolism. J. Clin. Microbiol. 41 (1), 506–508. https://doi.org/10.1128/JCM.41.1.506-508.2003.

Lee, C., Yang, W., Parr, R.G., 1988. Development of the Colle-Salvetti correlation-energy formula into a functional of the electron density. Phys. Rev. B 37 (2), 785–789. https://doi.org/10.1103/PhysRevB.37.785.

Liang, H., Xing, Y., Chen, J., Zhang, D., Guo, S., Wang, C., 2012. Antimicrobial activities of endophytic fungi isolated from Ophiopogon japonicus (Liliaceae). BMC Complement. Altern. Med. 12, 238. https://doi.org/10.1186/1472-6882-12-238.

Limban, C., Chifiriuc, M.-C., Missir, A.-V., Chiriţă, I., Bleotu, C., 2008. Antimicrobial Activity of Some New Thioureides Derived from 2-(4-Chlorophenoxymethyl)benzoic Acid. Molecules 13 (3), 567–580. https://doi.org/10.3390/molecules13030567.

Limban, C., Grumezescu, A.M., Saviuc, C., Voicu, G., Predan, G., Sakizlian, R., Chifiriuc, M.C., 2012. Optimized Anti-pathogenic Agents Based on Core/Shell Nanostructures and 2-((4-Ethylphenoxy)ethyl)-N-(substituted-phenylcarbamothioyl)-benzamides. Int. J. Mol. Sci. 13, 12584–12597. https://doi.org/10.3390/ijms131012584.

Limban, C., Marutescu, L., Chifiriuc, M.C., 2011. Synthesis, Spectroscopic Properties and Antipathogenic Activity of New Thiourea Derivatives. Molecules 16, 7593–7607. https://doi.org/10.3390/molecules16097593.

Mahmoud, H.K., Abbas, A.A., Gomha, S.M., 2020. Synthesis, Antimicrobial Evaluation and Molecular Docking of New Func-

tionalized Bis(1,3,4-Thiadiazole) and Bis(Thiazole) Derivatives. Polycycl. Aromat. Compd., 1–13 https://doi.org/10.1080/10406638.2019.1709085.

Monteiro, M.C., de la Cruz, M., Cantizani, J., Moreno, C., Tormo, J. R., Mellado, E., De Lucas, J.R., Asensio, F., Valiante, V., Brakhage, A.A., Latgé, J.-P., Genilloud, O., Vicente, F., 2012. A new approach to drug discovery: high-throughput screening of microbial natural extracts against Aspergillus fumigatus using resazurin. J. Biomol. Screen. 17 (4), 542–549. https://doi.org/10.1177/1087057111433459.

O'Donnell, F., Smyth, T.J.P., Ramachandran, V.N., Smyth, W.F., 2010. A study of the antimicrobial activity of selected synthetic and naturally occurring quinolines. Int. J. Antimicrob. Agents 35 (1), 30–38. https://doi.org/10.1016/j.ijantimicag.2009.06.031.

Oka, Y., Yabuuchi, T., Fujii, Y., Ohtake, H., Wakahara, S., Matsumoto, K., Endo, M., Tamura, Y., Sekiguchi, Y., 2012. Discovery and optimization of a series of 2-aminothiazole-oxazoles as potent phosphoinositide 3-kinase gamma inhibitors. Bioorg. Med. Chem. Lett. 22, 7534–7538. https://doi.org/10.1016/j.bmcl.2012.10.028.

Olar, R., Badea, M., Marinescu, D., Chifiriuc, M.-C., Bleotu, C., Grecu, M.N., Iorgulescu, E.-E., Lazar, V., 2010. N, N-dimethylbiguanide complexes displaying low cytotoxicity as potential large spectrum antimicrobial agents. Eur. J. Med. Chem. 45 (7), 3027–3034. https://doi.org/10.1016/j.ejmech.2010.03.033.

Ou, M., Zhu, C., Zhang, Q.-L., Zhu, B.-X., 2013. Synthesis and characterization of macrocyclic compounds with a hydroxyl functional group. Chinese Chem. Lett. 24 (10), 869–872. https://doi.org/10.1016/j.cclet.2013.06.014.

Potewar, T.M., Ingale, S.A., Srinivasan, K.V., 2007. Efficient synthesis of 2,4-disubstituted thiazoles using ionic liquid under ambient conditions: a practical approach towards the synthesis of Fanetizole. Tetrahedron 63, 11066–11069. https://doi.org/10.1016/j.tet.2007.08.036.

Priyadarshi, A., Kim, E.E., Hwang, K.Y., 2010. Structural insights into Staphylococcus aureus enoyl-ACP reductase (FabI), in complex with NADP and triclosan. Proteins Struct. Funct. Bioinforma. 78 (2), 480–486. https://doi.org/10.1002/prot.22581.

Rajanarendar, E., Ramakrishna, S., Murthy], K. [Rama, 2012. Synthesis of novel isoxazolyl bis-thiazolo[3,2-a]pyrimidines. Chinese Chem. Lett. 23, 899–902. https://doi.org/https://doi.org/10.1016/j.cclet.2012.06.029

Sayed, A.R., Gomha, S.M., Taher, E.A., Muhammad, Z.A., El-Seedi, H.R., Gaber, H.M., Ahmed, M.M., 2020. One-Pot Synthesis of Novel Thiazoles as Potential Anti-Cancer Agents. Drug Des. Devel. Ther. 14, 1363–1375. https://doi.org/10.2147/DDDT.S221263.

Verma, A., Saraf, S.K., 2008. 4-Thiazolidinone – A biologically active scaffold. Eur. J. Med. Chem. 43, 897–905. https://doi.org/10.1016/j.ejmech.2007.07.017.

Watanabe, M., Uesugi, M., 2013. Small-molecule inhibitors of SREBP activation – potential for new treatment of metabolic disorders. Med. Chem. Commun. 4, 1422–1433. https://doi.org/10.1039/C3MD00177F.

Zhao, B., Wu, Y.J., Tao, J.C., Yuan, H.Z., Mao, X.A., 1996. Studies on the syntheses of hydroxy-bearing benzo-azacrown ethers and their complexing behaviour. Polyhedron 15, 1197–1202. https://doi.org/10.1016/0277-5387(95)00262-6.